

Fab' fragments from different rabbits, which strongly inhibited neuron-neuron interaction (4), did not inhibit adhesion (Table 1, lower part), suggesting that the N-CAM present on the surface of these neurons is not involved in neuron-glia adhesion.

Although it is possible that inhibition by the Fab' fragments from antisera to brain membranes is due to nonspecific coating of the cell surface, this is an unlikely explanation because anti-N-CAM Fab' fragments had no effect on the adhesion, and N-CAM represents approximately 1 percent of the neuronal cell surface protein (4).

To address further the possibility that some form of N-CAM might be involved in neuron-glia adhesion, rabbits were immunized with a soluble fraction from brain membranes from which N-CAM antigens had been removed by affinity chromatography (4). The IgG fraction that was purified from these rabbit antisera recognized several proteins from brain membranes but did not recognize N-CAM by immunoblotting techniques (14). Preincubation of neurons with Fab' fragments from these antibodies reduced the number of neurons bound to monolayers of glial cells by 50 percent (Table 1). These results support the suggestion that N-CAM is not involved in adhesion between these neuronal and glial cells. Instead, it appears that antibodies against other neuronal cell surface molecules are responsible for the inhibition of neuron-glia adhesion. The identification and isolation of these molecules should permit a more detailed analysis of their relation to N-CAM, allow us to definitively exclude N-CAM as a ligand, and also permit the analysis of specific interacting molecules on the glial cell surface.

Although it is possible that the cells that specifically bind to monolayers of glial cells might represent a minor population of nonneuronal cells, this possibility seems unlikely because greater than 85 percent of the small round cells bound to the monolayer were N-CAM-positive by indirect immunofluorescence, indicating that they are neuronal cells and not glial cells. In view of the fact that N-CAM has not been seen on the surface of glial cells in culture, the possibility that glia-glia adhesion contributes in a major fashion to the counts of bound cells is unlikely.

In summary, adhesion was measured between embryonic chick neuronal and glial cells, each of which was identified by a different specific monoclonal antibody. Polyspecific rabbit antibodies to neuronal cell determinants have been obtained that block calcium-independent

adhesion between neuronal and glial cells in vitro. The inhibitory activity of these antibodies cannot be attributed to the presence of anti-N-CAM. The results indicate that a specific mechanism mediates adhesion between neuronal and glial cells and suggest that neuronal cell surface antigens different from N-CAM are responsible for heterotypic cell-cell adhesion. This hypothesis could be tested by identifying specific cell surface molecules that neutralize the ability of Fab' fragments against brain membranes to inhibit neuron-glia adhesion.

M. GRUMET  
U. RUTISHAUSER  
G. M. EDELMAN

Rockefeller University,  
New York 10021

#### References and Notes

1. S. S. Varon and G. G. Somjen, *Neurosci. Res. Prog. Bull.* **17**, 1 (1979).
2. P. Rakic, in *Brain Mechanisms in Mental Retardation*, N. A. Buchwald and M. Brazier, Eds. (Academic Press, New York, 1975), pp. 3-40.
3. G. M. Edelman, *Science* **219**, 450 (1983).
4. R. Brackenbury, J.-P. Thiery, U. Rutishauser, G. M. Edelman, *J. Biol. Chem.* **252**, 6835 (1977);
5. B. T. Walther, R. Ohman, S. Roseman, *Proc. Natl. Acad. Sci. U.S.A.* **70**, 1569 (1973).
6. R. Brackenbury, U. Rutishauser, G. M. Edelman, *ibid.* **78**, 387 (1981).
7. M. Sensenbrenner and P. Mandel, *Exp. Cell Res.* **87**, 159 (1974); B. Foucaud, R. Reeb, M. Sensenbrenner, G. Gombos, *ibid.* **137**, 285 (1982).
8. M. Grumet, U. Rutishauser, G. M. Edelman, *Nature (London)* **295**, 639 (1982).
9. D. R. Buskirk, J.-P. Thiery, U. Rutishauser, G. M. Edelman, *ibid.* **285**, 488 (1980); U. Rutishauser and G. M. Edelman, *J. Cell Biol.* **87**, 370 (1980); U. Rutishauser, M. Grumet, G. M. Edelman, *ibid.* **97**, 145 (1983).
10. U. Rutishauser, J.-P. Thiery, R. Brackenbury, G. M. Edelman, *J. Cell Biol.* **79**, 371 (1978).
11. K. D. McCarthy and L. M. Partlow, *Brain Res.* **114**, 391 (1976); R. Adler, M. Manthorpe, S. Varon, *Dev. Biol.* **69**, 424 (1979).
12. M. Grumet, J.-P. Thiery, G. M. Edelman, unpublished observations.
13. W. Frazier and L. Glaser, *Annu. Rev. Biochem.* **48**, 491 (1979); G. Gerisch, *Curr. Top. Dev. Biol.* **14**, 243 (1980).
14. H. Towbin, T. Staehelin, J. Gordon, *Proc. Natl. Acad. Sci. U.S.A.* **76**, 4350 (1979).
15. Supported by NIH grants HD-16550, HD-09635, AI-11378, AM-04256, and a postdoctoral fellowship to M.G. AI-06414. We thank H. Hjelt and S. Igdaloff for technical assistance.

13 July 1983

## In vivo Determination of the Pyridine Nucleotide Reduction Charge by Carbon-13 Nuclear Magnetic Resonance Spectroscopy

**Abstract.** *An intracellular coenzyme has been observed by carbon-13 nuclear magnetic resonance spectroscopy. The pyridine nucleotides in Escherichia coli were specifically labeled with carbon-13 from the biosynthetic precursor, nicotinic acid. The intracellular redox status and metabolic transformations of the pyridine nucleotides were examined under a variety of conditions. A highly reduced nicotinamide adenine dinucleotide pool was observed under anaerobic conditions only in cells that were cultured aerobically on glycerol.*

Since the initial use of isotopic labeling in combination with nuclear magnetic resonance (NMR) detection to study glucose metabolism by yeast cells (1), applications of NMR for in vivo metabolic studies have been extended to a wide variety of microorganisms, cells, perfused organs, and, most recently, intact animals (2). In general, the focus of these studies has been on metabolic regulation, since in most instances the pathways involved have been established for some time. In <sup>13</sup>C labeling studies, information pertinent to metabolic regulation may be obtained by direct observation of time-dependent signal intensities, direct observation of metabolic intermediates, and analysis of label distributions and multiplet intensities in the various metabolites (3). In parallel with the development of <sup>13</sup>C NMR for in vivo metabolic analysis, <sup>31</sup>P NMR has been shown to provide useful data on metabolic regulation in terms of intracellular pH and phosphonucleotide energy charge (4). Si-

multaneous <sup>13</sup>C and <sup>31</sup>P NMR detection appears to represent a very promising avenue for detailed studies of metabolic regulation in vivo (5). We report here the application of <sup>13</sup>C labeling and NMR detection to the study of an intracellular coenzyme pool, the pyridine nucleotides.

The redox status of the di- and triphosphopyridine nucleotide pools is an important regulatory parameter. Concentrations of important metabolic intermediates such as pyruvate-lactate, and metabolic flux through critical branching steps have been proposed to be dependent on the redox status of these two pools (6). Anderson and von Meyenburg (7) have suggested a convenient quantitative characterization of the status of these pools as the catabolic reduction charge (CRC),  $[NADH]/([NADH] + [NAD^+])$ , and the anabolic reduction charge (ARC),  $[NADPH]/([NADPH] + [NADP^+])$ , where NAD<sup>+</sup> is nicotinamide adenine dinucleotide and NADP<sup>+</sup>

is nicotinamide adenine dinucleotide phosphate. Although CRC and ARC are typically quite different, meaningful analysis can be carried out even if only a weighted average reduction charge can be determined, as is the case for the *in vivo* fluorescence measurements developed by Chance and co-workers (8). In this context, it is convenient to define a mean reduction charge (MRC),  $([NADH] + [NADPH])/[\text{total pyridine nucleotides}]$  (9). Since the approach described here involves labeling the intracellular pyridine nucleotide pool in the nicotinamide moiety, and since the nicotinamide chemical shifts are sensitive to the redox status but not to the presence of the remote phosphoryl group, which distinguishes the di- and triphosphopyridine nucleotides (10), the NMR characterization will in general yield only an MRC value. However, in contrast to fluorescence measurements, signals corresponding to oxidized pyridine nucleotides as well as to other metabolites can be directly observed.

To demonstrate the feasibility of this approach, we labeled the pyridine nucleotides of *Escherichia coli* from the biosynthetic precursor nicotinic acid. A nicotinic acid-requiring strain of *E. coli* (ATCC 23788) was cultured on a minimal medium (11) containing nicotinic acid (0.5 mM) labeled with  $^{13}\text{C}$  at either the carboxyl (C-7) or C-2 position (12). The cells were harvested in the exponential growth phase, washed to remove extracellular nicotinic acid, and resuspended at a density of approximately  $10^{11}$  cells per milliliter in phosphate buffer (pH 7.2) with or without a carbon source. Cells were oxygenated in the spectrometer by using a specially designed dual capillary system mounted concentrically with the magnet bore. Oxygen was bubbled at a low rate (20 to 30 ml/min) near the bottom of the NMR tube through one capillary and at a higher rate (150 ml/min) above the detection coil through the outer capillary (13). Under these conditions, cells glycolyzing D-[1- $^{13}\text{C}$ ]glucose did not produce significant quantities of L-[3- $^{13}\text{C}$ ]lactate. Proton-decoupled  $^{13}\text{C}$  NMR spectra were obtained at 75.5 MHz in a Bruker WM 300 wide-bore spectrometer by using a Cryomagnet Systems 20-mm probe. The C-2 label was chosen because resonances for both oxidized and reduced pyridine nucleotides occur at about 140 ppm, a relatively uncrowded region of the whole-cell  $^{13}\text{C}$  spectrum, and because the protonated carbon was anticipated to have a short spin lattice relaxation time ( $T_1$ ), minimizing intensity distortions arising from overpulsing (14). An inversion-recovery experiment was

carried out at 19°C to estimate the  $T_1$  value for the nicotinamide C-2 carbon of  $\text{NAD}^+$  (under conditions for which the  $\text{NAD}^+$  concentration is relatively invariant), and a value of  $\sim 300$  msec was obtained. Even allowing for a twofold increase in  $T_1$  at 25°C, the  $T_1$  value will be sufficiently short to ensure that resonance intensities will not be distorted by overpulsing.

Initial studies were carried out to assess the effects of oxygen deprivation on the MRC. Figure 1 shows part of the  $^{13}\text{C}$  NMR spectrum of harvested *E. coli* cultured on D-glucose under aerobic conditions in the presence of [2- $^{13}\text{C}$ ]nicotinate and observed under anaerobic conditions. The spectrum contains two resonances that correspond to free nicotinate (151.5 ppm) and to oxidized pyridine nucleotide (142.6 ppm), the latter representing a superposition of signals corresponding to  $\text{NAD}^+$ ,  $\text{NADP}^+$ , and nicotinamide mononucleotide ( $\text{NMN}^+$ ) (if present). In general, the levels of free nicotinate were negligible immediately after harvest, but tended to increase with time, the rate of increase being a strong function of temperature. Catabolism of the pyridine nucleotides to nicotinic acid

in the absence of oxygen and an energy source is expected on the basis of the pyridine nucleotide cycle (15), although it was recently reported that the predominant flux in *E. coli* bypasses both nicotinamide and nicotinic acid due to the direct conversion of  $\text{NMN}^+$  to nicotinate mononucleotide (16). The present results also differ from those reported under conditions of nicotinic acid starvation, in which nicotinate mononucleotide rather than nicotinate was shown to accumulate (17). No signals corresponding to reduced pyridine nucleotides were observed with the cells grown on glucose. This result was invariant with respect to change in oxygenation state, addition of ethanol, presence of glucose during the experiment, and growth under anaerobic conditions. The long accumulation time (5 hours) indicated in Fig. 1 was carried out to yield a maximum MRC value of 0.04.

Reports in the literature on the response of the pools to oxygen levels appear to vary considerably (7, 18, 19). Fluorescence studies on *Klebsiella aerogenes* *in vivo* indicate that a decrease in the availability of oxygen is associated with a rapid rise in the MRC; however,

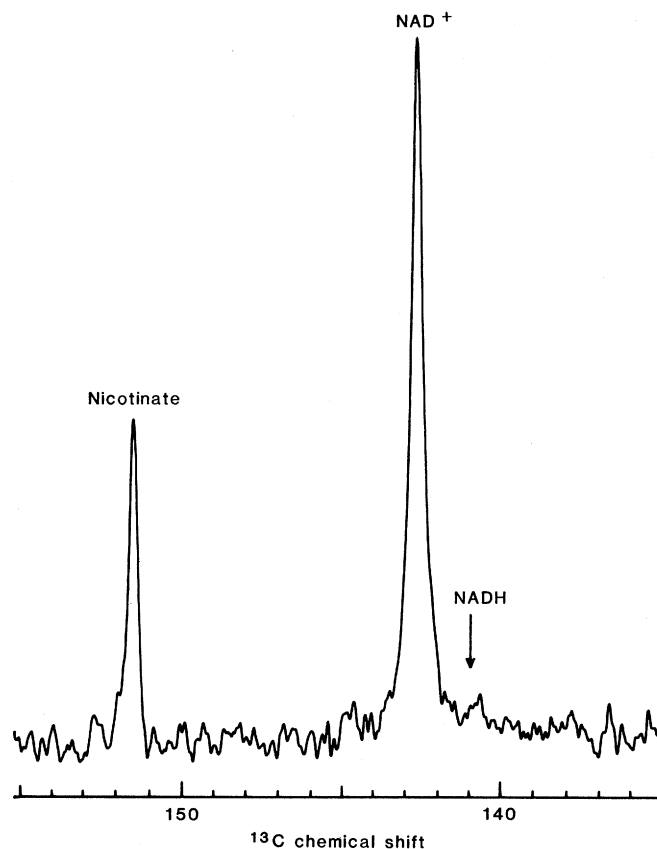


Fig. 1. Proton-decoupled  $^{13}\text{C}$  NMR spectrum of nicotinic acid-requiring *E. coli* cultured on a medium containing [2- $^{13}\text{C}$ ]nicotinic acid. Resonances corresponding to free nicotinate and to oxidized pyridine nucleotide are indicated, and the arrow indicates the position of the reduced pyridine nucleotide resonance. The head of the arrow corresponds to 10 percent of the height of the oxidized peak. Spectra were obtained at approximately 25°C by using the following acquisition parameters: 16 kHz spectral width, 16 K data points in the free induction decay  $90^\circ$  observation pulse, and a recycle time of 2.141 seconds. The proton broadband decoupler was centered at 8.2 ppm in the proton spectrum and a bilevel

decoupling scheme was used with 10 W of forward power during the acquisition, 0.5 W during the delay, and a duty cycle of 0.25. Spectra were averaged in 30-minute blocks, and this spectrum represents a sum of ten 30-minute accumulations. Improvement in the signal-to-noise ratio was achieved by using a 3-Hz exponential broadening function. Chemical shifts are reported in parts per million downfield from sodium 3-trimethylsilylpropionate-2,2,3,3- $\text{d}_4$  (TSP, Merck).

extraction of the nucleotides indicates that this change corresponds to a relatively small change in the magnitude of the MRC (18). Anderson and von Meyenburg (7), using a radioassay method based on [carboxyl- $^{14}\text{C}$ ]nicotinate, found negligible short-term changes in the ARC and CRC, but a gradual long-term decrease in the ARC. In contrast, Wimpenny and Firth (19) reported dramatic short-term (< 1 minute) changes both in the total levels of diphosphopyridine nucleotides and in the CRC in *K. aerogenes* and *E. coli*. These differences may reflect differences in the various growth parameters; however, the present results appear to be more consistent with the first two studies, and suggest problems in the methodology used by Wimpenny and Firth. The maximum MRC value obtained under the conditions reported above is, however, surprisingly low compared with literature values. This may reflect (i) selective broadening of the reduced pyridine nucleotide resonance due to chemical exchange with enzyme binding sites or the oxidized form; (ii) selective broadening of the NADPH resonance, which should contribute significantly to the total reduced resonance; (iii) resonances from oxidized pyridine nucleotides that do not reflect the metabolically available pool

but an unavailable or "storage" NAD pool, as has been proposed to exist in mammalian liver (20); or (iv) errors in the literature values reflecting artifacts of the extraction process.

Although complete analysis of all the above factors will require considerable time, efforts were made to create conditions leading to a highly reduced MRC. This condition was achieved by aerobic growth of the cells on a glycerol carbon source, followed by NMR analysis under anaerobic conditions. While *E. coli* will grow on glucose, it will not grow when glycerol is used as the sole source of carbon and energy in the absence of an exogenous hydrogen acceptor such as fumarate or nitrate (21). This reflects the fact that in the anaerobic conversion of glucose to lactate both precursor and product are at the same oxidation state, while in the anaerobic oxidation of glycerol to lactate one equivalent of  $\text{NAD}^+$  is consumed. With this approach, a significant, time-dependent increase in the MRC was observed (Fig. 2). These results indicate that if sufficient NADH and NADPH are present, the exchange between oxidized and reduced pyridine nucleotides is not sufficiently rapid to collapse the resonances.

The method proposed here should find general utility in NMR studies of meta-

bolic regulation. Spectra of cell suspensions with adequate signal-to-noise ratios can be obtained in 30 minutes (Fig. 2), although in general this will depend on the MRC value being measured. Greater sensitivity is available for studies of whole organs (22). Although the NMR method offers significantly lower sensitivity than fluorescence measurements for in vivo detection of pyridine nucleotides, it enables (i) observation of reduced and oxidized nucleotides as well as other metabolites, such as free nicotinate; (ii) observations in cells containing other fluorescent molecules that would interfere with the reduced pyridine nucleotide determination; (iii) selective observation of the free nucleotide pool, which is important in metabolic regulation and which contrasts with the fluorescent determination in which enzyme-complexed pyridine nucleotides can be more fluorescent; and (iv) simultaneous observation of the metabolic flux with  $^{13}\text{C}$ -labeled metabolites and the MRC based on a labeled nicotinate precursor. The latter factor is perhaps most significant, and the possibility of correlating the MRC with the metabolic flux may provide a more complete description of metabolic conversions than has been available.

CLIFFORD J. UNKEFER  
RICHARD M. BLAZER  
ROBERT E. LONDON

Los Alamos National Laboratory,  
Los Alamos, New Mexico 87545

#### References and Notes

- R. T. Eakin, L. O. Morgan, C. T. Gregg, N. A. Matwyoff, *FEBS Lett.* **28**, 259 (1973).
- R. S. Norton, *Bull. Magn. Reson.* **3**, 29 (1980); R. G. Shulman *et al.*, *Science* **205**, 160 (1979); N. A. Matwyoff, R. E. London, J. Y. Hutson, *Am. Chem. Soc. Symp. Ser.* **191** (1982), pp. 157-186.
- R. E. London, V. H. Kollman, N. A. Matwyoff, *J. Am. Chem. Soc.* **97**, 3565 (1975); T. E. Walker, C. H. Han, V. H. Kollman, R. E. London, N. A. Matwyoff, *J. Biol. Chem.* **257**, 1189 (1982).
- D. P. Hollis, in *Biological Magnetic Resonance*, L. J. Berliner and J. Reuben, Eds. (Plenum, New York, 1980), pp. 1-44; D. I. Hoult *et al.*, *Nature (London)* **252**, 285 (1974).
- P. Styles, C. Grathwohl, F. F. Brown, *J. Magn. Reson.* **35**, 329 (1979).
- H. A. Krebs, *Adv. Enzyme Reg.* **6**, 468 (1968); L. L. Madison, *Adv. Metab. Disord.* **3**, 85 (1968); R. L. Vecch, in *Microenvironments and Metabolic Compartmentation*, P. A. Srere and R. W. Estabrook, Eds. (Academic Press, New York, 1978), pp. 17-64; J. Bautista, J. Satrustegui, A. Machado, *FEBS Lett.* **105**, 333 (1979).
- K. B. Anderson and K. von Meyenburg, *J. Biol. Chem.* **252**, 4151 (1977).
- B. Chance *et al.*, in *Microenvironments and Metabolic Compartmentation*, P. A. Srere and R. W. Estabrook, Eds. (Academic Press, New York, 1978), pp. 131-148; B. R. Masters, B. Chance, J. Fischberg, in *Noninvasive Probes of Tissue Metabolism*, J. S. Cohen, Ed. (Wiley, New York, 1982), pp. 79-118 and references therein.
- The MRC is related to the ARC and CRC as follows:  $\text{MRC} = [\text{CRC} + R(\text{ARC})]/(1 + R)$ , where  $R = ([\text{NADPH}] + [\text{NADP}^+])/([\text{NADH}] + [\text{NAD}^+])$  and is the ratio of tri- to diphosphopyridine nucleotides. On the basis of values reported by Anderson and von Meyenburg (7), typical MRC values range from 0.1 to 0.2.

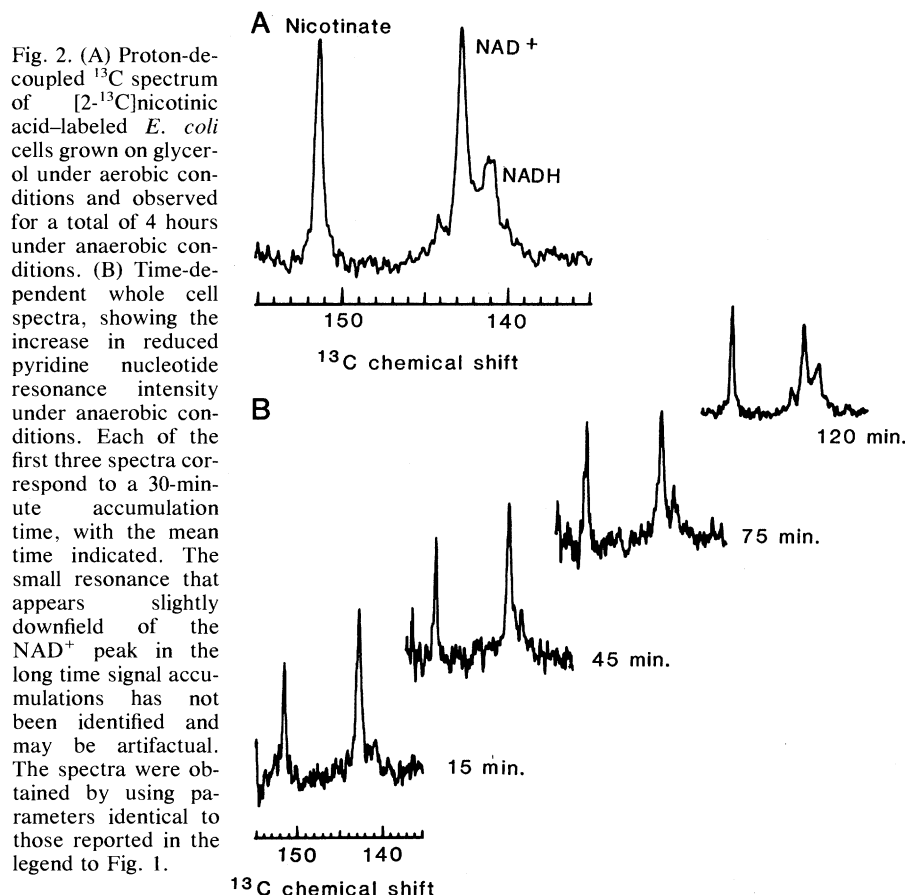


Fig. 2. (A) Proton-decoupled  $^{13}\text{C}$  spectrum of [2- $^{13}\text{C}$ ]nicotinic acid-labeled *E. coli* cells grown on glycerol under aerobic conditions and observed for a total of 4 hours under anaerobic conditions. (B) Time-dependent whole cell spectra, showing the increase in reduced pyridine nucleotide resonance intensity under anaerobic conditions. Each of the first three spectra correspond to a 30-minute accumulation time, with the mean time indicated. The small resonance that appears slightly downfield of the  $\text{NAD}^+$  peak in the long time signal accumulations has not been identified and may be artifactual. The spectra were obtained by using parameters identical to those reported in the legend to Fig. 1.

10. B. Birdsall and J. Feeney, *J. Chem. Soc. Perkin Trans. 2* (1972), p. 1643.
11. B. D. Davis and M. Mingioli, *J. Bacteriol.* **17**, 60 (1950).
12. M. C. Meinert, H. A. Nunez, R. U. Byerrum, *J. Labelled Compd.* **14**, 893 (1978); T. A. Bryson, J. C. Wisowaty, R. B. Dunlap, R. R. Fisher, P. D. Ellis, *J. Org. Chem.* **39**, 3436 (1974).
13. K. Ugurbil, H. Rottenberg, P. Glynn, R. G. Shulman, *Biochemistry* **21**, 1068 (1982).
14. J. R. Lyerla, Jr., and G. C. Levy, in *Topics in Carbon-13 NMR Spectroscopy*, G. C. Levy, Ed. (Wiley, New York, 1974), vol. 1, p. 79.
15. A. J. Andreoli, T. W. Okita, R. Bloom, T. A. Grover, *Biochem. Biophys. Res. Commun.* **49**, 264 (1972).
16. D. Hillyard *et al.*, *J. Biol. Chem.* **256**, 8491 (1981).
17. R. Lundquist and B. M. Olivera, *ibid.* **248**, 5137 (1973).
18. D. E. F. Harrison and B. Chance, *Appl. Microbiol.* **19**, 446 (1970).
19. J. W. T. Wimpenny and A. Firth, *J. Bacteriol.* **111**, 24 (1972).
20. C. Bernofsky, *Mol. Cell. Biochem.* **33**, 135 (1980).
21. E. C. C. Lin, *Annu. Rev. Microbiol.* **30**, 535 (1976).
22. S. M. Cohen, R. Rognstad, R. G. Shulman, J. Katz, *J. Biol. Chem.* **256**, 3428 (1981).
23. This work was supported in part by an NIH National Research Service Award F32 HL06262 (C.J.U.) and was performed under the auspices of the Department of Energy.

22 October 1982; revised 11 March 1983

## Type II Collagen-Induced Autoimmune Endolymphatic Hydrops in Guinea Pig

**Abstract.** *Endolymphatic hydrops was induced in guinea pigs by immunizing them with native bovine type II collagen. Histopathologic changes consisted of moderate extension of the Reissner's membrane, spiral ganglion degeneration, atrophied organ of Corti, and mild atrophy of the surface epithelium in the endolymphatic duct. These findings suggest that an immune response directed against type II collagen—a type of collagen found in the membranous labyrinth, subepithelial layer of the endolymphatic duct, spiral ligament, and enchondral layer of the otic capsule—may induce endolymphatic hydrops.*

In 1861, a Paris physician, Prosper Ménière, described an illness characterized by vertigo, deafness, and tinnitus (1). This disease, the cause of which is still unknown, has been linked to a failure of the mechanism regulating the production and disposal of endolymph. The occurrence of endolymphatic hydrops in the ears of animals with bacterial labyrinthitis was recognized as early as 1926 by Wittamaac (2). Most of the occurrences were spontaneous and reflected the inflammatory reaction of the epithelial lining of the endolymphatic space (2, 3). Various methods have been used to induce endolymphatic hydrops in animals, including intravenous injection of horse serum (4), tubercle bacilli (4), egg albumin (5), or horseradish peroxidase (6); injection of human serum through the stylomastoid foramen has also been used (7). Other methods include surgical obstruction of endolymphatic duct (8, 9), injection of ethacrynic acid (10), and infrasound acoustic trauma (11). The immunologic methods, although better than the surgical methods, produced only limited success.

We described autoimmune hearing loss, vestibular dysfunction, and otospongiotic lesions in the rat (12, 13). In addition, we studied guinea pigs for the occurrence of the inner ear lesions (14). All of the abnormalities appeared to be associated with autoimmunity to type II collagen. Antibody titers to type II collagen were higher in the patients with Ménière's disease than in controls, an

indication that autoimmunity to type II collagen might have a role in the etiology of Ménière's disease (15).

It was, therefore, of interest to develop a well-defined animal model of autoimmune endolymphatic hydrops by immunization with type II collagen. We have now developed such a model in guinea pigs. Bovine type II collagen was isolated and purified as described (16). The purity of the collagen preparations was determined by amino acid analysis, sodium dodecyl sulfate-polyacrylamide gel electrophoresis, and uronic acid analysis (16). In each case, there was no detectable contamination by noncollagenous proteins, by proteoglycans, or by other types of collagen.

Collagen for immunization was stirred overnight in 0.1N acetic acid at 4°C. An emulsion was made by adding collagen to an equal volume of incomplete

Freund's adjuvant and homogenizing the mixture (VirTis homogenizer). Hartley guinea pigs received intradermal injections (into the footpad) of 400 µg of native bovine type II collagen emulsified with incomplete Freund's adjuvant. All of the guinea pigs were given boosters of an identically prepared emulsion injected into the foot at 7-day intervals.

Serums were collected by cardiac puncture and antibody titers were assayed by an enzyme-linked immunosorbent assay (ELISA) method (17). Disposable polystyrene 96-well microtiter plates were coated with collagen dissolved in 0.4M ionic strength phosphate buffer (pH 7.6). Collagen-coated plates were incubated with tris-NaCl containing 1 percent bovine serum albumin (BSA) to block nonspecific binding. Serum, diluted 1:100 and 1:1000 in tris-NaCl containing 1 percent BSA and 0.05 percent Tween 20, was added to the plates, which were then incubated at room temperature for 2 hours. The plates were washed, and peroxidase-conjugated goat antiserum to guinea pig immunoglobulin G (IgG) (Cappel Laboratory, Inc., Cochranville, Pennsylvania) was added at a predetermined dilution. After a 2-hour incubation at room temperature, the plates were washed three times, and 100 µl of orthophenylene diamine (OPD) substrate (25 mg of OPD in 25 µl of 30 percent H<sub>2</sub>O<sub>2</sub> in phosphate citrate buffer, pH 5). Sixty minutes later, the colorimetric reaction was read at 490 nm (Dynatec MR 580 micro-ELISA auto-reader). Analyses were performed in duplicate, and the results were expressed as absorbance.

The inner ear fluid was collected as follows: the thoracic cavity of the anesthetized animal was opened and the blood was removed from the heart. In order to avoid blood contamination of the inner ear fluid and cerebrospinal fluid, we perfused the animals through the left ventricle of the heart with physiological saline. The cerebrospinal fluid was

Table 1. Histologic changes in the inner ear of 13 guinea pigs immunized with type II collagen. Changes were characterized as profound (+++), moderate (++), or slight (+). A dash indicates a normal condition.

Changes	Finding in animals			
	Killed 2 weeks after last immunization		Killed 4 weeks after last immunization	
	N = 1	N = 3	N = 2	N = 7
Hydrops	++	+	+	—
Degeneration of organ of Corti	++	++	++	+
Precipitation in cochlear duct	++	++	+	+
Degeneration of spiral ganglion	++	+	—	—
Dilation of endolymphatic duct and sac	+	+	+	—